Publishing Excellence
Inspiring Progress
ARISTON PUBLICATIONS

MatSci Express

ISSN: 2997-8440 www.aristonpubs.com/matsci-express https://doi.org/10.69626/mse.2025.0207

RESEARCH ARTICLE

Enhanced Surface Performance of AISI–201 Austenitic Stainless Steel and Copper via Low–Temperature Aluminum Cathodic Cage Plasma Nitriding

Muhammad Bilal Khalid[1], Syed Salman Hussain[1,*], Muhammad Shafiq[2], Muhammad Asghar[2], Shahid Hussain[3,4,*]

ABSTRACT: Cathodic cage plasma nitriding (CCPN) is a well-established and economically viable surface engineering technique renowned for enhancing the properties of metallic materials. This study specifically investigates the pivotal role of processing temperature within the CCPN system, focusing on its impact on AISI-201 austenitic stainless steel and copper. Samples of both materials were treated using an aluminum cathodic cage at a temperature of 300°C for a duration of four hours. The modified surface layers were subjected to a comprehensive suite of analyses, including X-ray diffraction (XRD), scanning electron microscopy (SEM), energy dispersive X-ray spectroscopy (EDS), Vickers microhardness testing, ball-on-disc wear testing, and potentiodynamic polarization corrosion analysis. The results demonstrated a substantial improvement in surface properties. XRD analysis confirmed the successful formation of a complex nitride layer, identifying phases such as AlN, CrN, FeN, and FeMnN on AISI-201, and AlN, Cu_3N, CuN_3, CuN_6, and $AlCu_4$ on copper. This microstructural evolution directly contributed to a remarkable 300% increase in surface hardness for both materials. Consequently, the wear resistance was significantly enhanced, evidenced by reduced wear track width and a lower coefficient of friction. The corrosion resistance in a 3.5% NaCl solution also showed marked improvement for the nitrided samples. This work provides a thorough explanation of the reaction mechanisms within the aluminum CCPN system and successfully correlates the findings with existing literature, underscoring the effectiveness of this method for low-temperature surface enhancement of challenging materials.

Keywords: Plasma nitriding, Wear resistance, Corrosion behavior, Surface hardening, Austenitic stainless steel, Copper.

Received: 23 January 2025; Revised: 28 April 2025; Accepted: 17 May 2025; Published Online: 09 June 2025

1. INTRODUCTION

Austenitic stainless steels represent a critical class of materials in modern engineering, prized for their exceptional combination of formability, toughness, and corrosion resistance. These properties make them indispensable across a diverse range of industries, from chemical processing plants and nuclear reactors to medical devices and architectural applications [1, 2]. The fundamental appeal of these steels lies in their austenitic face-centered cubic (fcc) crystal structure, which is primarily stabilized by nickel. Traditionally, the 300 series steels, characterized by their chromium-nickel (Cr-Ni) composition, have dominated these applications due to their renowned performance, particularly

[1] Department of Physics, International Islamic University, Islamabad, 44000, Pakistan.
[2] Department of Physics, Quaid-i-Azam University, Islamabad, 45320, Pakistan
[3] School of Materials Science and Engineering, Jiangsu University, Zhenjiang, 212013, China
[4] Department of Physics, University of Sargodha, Sargodha 40100, Pakistan

* Author to whom correspondence should be addressed:
salman.hussain@iiu.edu.pk (S. Salman Hussain)
shahid@ujs.edu.cn (Shahid Hussain)

© Ariston Publications 2025. All rights reserved.

in corrosive environments [3]. However, the high and volatile cost of nickel has driven the development of alternative, more economical grades. This economic pressure led to the creation of the 200 series stainless steels, which substitute a significant portion of the expensive nickel with manganese and nitrogen [4, 5]. AISI 201 is a prominent example of this series, offering a cost-effective solution for a variety of structural and decorative purposes.

Despite its economic advantage, the altered chemical composition of AISI 201 introduces significant material limitations. The reduced nickel and chromium content compared to 300 series steels results in a corresponding decrease in corrosion resistance, making it more vulnerable to pitting, crevice corrosion, and stress corrosion cracking in aggressive environments [6, 7]. Furthermore, its relatively low hardness and poor wear resistance severely restrict its use in applications involving mechanical abrasion, friction, or high load-bearing requirements [8-10]. These shortcomings have created a pressing need to develop effective surface engineering techniques that can enhance the surface-dependent properties of AISI 201 without compromising its bulk characteristics or economic appeal.

A similar challenge exists for copper and its alloys. Copper is a metal of immense industrial importance, foundational to electrical engineering, electronics, and thermal management systems due to its superior electrical and thermal conductivity [11-14]. However, its widespread application is often limited by its inherent mechanical shortcomings: it is exceptionally soft, exhibits poor wear resistance, and has a low yield strength [11, 12]. These disadvantages preclude its use in mechanical components subject to friction, abrasion, or high contact stresses. While bulk strengthening through alloying or work hardening is possible, these methods often detrimentally impact its prized electrical conductivity. Therefore, enhancing the surface mechanical properties of copper through a engineered surface layer, while preserving the conductive bulk, presents a highly attractive solution [11, 13].

Various surface modification techniques have been explored to address these issues. Conventional methods like DC plasma nitriding (DCPN) have been used for decades to harden ferrous metals. However, when applied to austenitic stainless steels like AISI 201, DCPN presents serious drawbacks. The process often leads to the formation of a discontinuous and brittle layer known as the "edge effect," where intense localized heating causes uneven treatment and can precipitate chromium nitrides at the grain boundaries. This chromium nitride formation depletes the surrounding matrix of chromium, the very element responsible for the steel's corrosion resistance, thereby severely degrading its protective passive layer [2, 15]. For copper, the challenge is even more fundamental; conventional nitriding techniques are notoriously inefficient due to copper's low nitrogen solubility and high diffusion activation energy, making the formation of a thick, hard nitride layer exceptionally difficult [12, 13].

The limitations of these traditional methods have spurred the development of advanced plasma technologies. Among these, Cathodic Cage Plasma Nitriding (CCPN) has emerged as a superior and innovative alternative. The CCPN system ingeniously reconfigures the plasma setup by placing the samples inside a cathodically biased cage, rather than making them the direct cathode. This cage, often made from a material like aluminum or iron, becomes the active source of sputtered species. The mechanism involves intense sputtering from the inner walls of the cage due to ion bombardment. These sputtered atoms then diffuse through the plasma, interacting with active nitrogen species, and subsequently deposit onto the sample surfaces, where they form a hard, uniform nitride layer [16-18]. This design effectively eliminates the detrimental edge effects and arc discharges associated with DCPN, ensures exceptional temperature uniformity across the workload, and allows for precise control over the chemical composition of the deposited layer by simply changing the cage material [19-21]. The aim of this study was to improve surface characteristics of AISI-201 and copper in terms of hardness, corrosion and wear at low temperature. In current study, the effect of low temperature i.e. 300°C CCPN has studied with fixed 4 hours duration on the surface of AISI-201 and copper.

The novelty of this paper lies in the innovative application of a dedicated aluminum cathodic cage for the simultaneous low-temperature (300°C) plasma nitriding of two notoriously difficult-to-nitride materials: AISI 201 austenitic stainless steel and pure copper. This approach bypasses the inherent limitations of conventional nitriding for these metals. For AISI 201, the process avoids the chromium depletion and associated corrosion resistance loss typical of DCPN by depositing a dominant layer of aluminum nitride (AlN). For copper, it overcome's the metal's innate resistance to nitriding by actively depositing pre-formed aluminum and copper nitrides onto its surface, a feat not efficiently achievable by traditional methods. This single, efficient process successfully enhances hardness, wear resistance, and corrosion performance in both materials, representing a significant advancement in surface engineering methodology.

2. EXPERIMENTAL DETAILS

2.1. Sample Preparation

Square specimens of AISI-201 austenitic stainless steel and commercially pure copper (Cu) were sectioned to dimensions of 20 mm × 20 mm × 5 mm. The samples were subsequently subjected to a meticulous grinding process using a sequential series of silicon carbide abrasive papers, commencing with a coarse 220 grit and progressively advancing through finer grits up to 2000. Following grinding, the samples were mirror-polished using a 0.3 µm alumina (Al_2O_3) suspension to achieve an optically flat, scratch-free surface finish. To remove any residual polishing contaminants and organic matter, all specimens were ultrasonically cleaned in an acetone bath for a duration of 15 minutes and then thoroughly dried in a stream of warm air prior to any treatment or

 © Ariston Publications 2025. All rights reserved.

analysis.

2.2. Cathodic Cage Plasma Nitriding (CCPN) Treatment

The surface modification was performed using a custom-designed Cathodic Cage Plasma Nitriding (CCPN) reactor. The cathodic cage was fabricated from pure aluminum (Al 1100) and featured a symmetrical arrangement of holes to ensure uniform plasma distribution. The meticulously prepared AISI-201 and copper samples were placed on the sample holder, which was electrically insulated from the cathodic cage, ensuring they were maintained at a floating potential throughout the process. The nitriding treatment was conducted at a sustained temperature of 300 °C (± 5 °C) for a constant duration of 4 hours. The process atmosphere consisted of a gaseous mixture of 25% nitrogen (N_2) and 75% hydrogen (H_2), maintained at a total working pressure of 3.0 mbar. The DC power supply was operated at a voltage of 500 V to sustain the plasma discharge. The specific details of the plasma generation and the sputter-deposition mechanism within this CCPN configuration have been extensively documented in prior publications [15-22].

2.3. Microstructural and Morphological Characterization

The phase constitution of both untreated and nitrided samples was identified using X-ray diffraction (XRD) analysis. The measurements were performed on a Panalytical X'Pert Pro diffractometer equipped with a Cu Kα radiation source (wavelength λ = 1.5406 Å), operated at an accelerating voltage of 40 kV and a filament current of 30 mA. Data was collected in a Bragg-Brentano geometry over a 2θ range of 20° to 80° with a step size of 0.02°. The surface morphology and topography of the treated layers were examined using a Carl Zeiss EVO MA10 scanning electron microscope (SEM). Complementary chemical analysis and elemental distribution maps were acquired using an Oxford Instruments X-Max energy dispersive X-ray spectroscopy (EDS) detector attached to the SEM.

2.4. Mechanical and Tribological Testing

The microhardness profiles of the cross-sectional and surface layers were evaluated using a Wilson Wolpert 402 MVD Vickers microhardness tester. Measurements were taken under applied loads ranging from 25 gf to 1000 gf, with a dwell time of 15 seconds. Each reported hardness value represents the average of at least five indents to ensure statistical reliability. The tribological performance, specifically the wear resistance and coefficient of friction, was assessed using a Ducom TR-20 ball-on-disc tribometer. Tests were conducted under a normal load of 10 N, with a 6 mm diameter tungsten carbide (WC) ball as the counterface, a sliding speed of 0.1 m/s, and a total sliding distance of 1000 m. The wear track morphology and volumetric wear loss were subsequently quantified using SEM imaging and profilometry.

2.5. Electrochemical Corrosion Analysis

The electrochemical corrosion behavior was investigated at room temperature using a Gill AC potentiostat from ACM Instruments. A standard three-electrode electrochemical cell configuration was employed, comprising the sample as the working electrode (with an exposed area of 1 cm^2), a platinum mesh as the counter electrode, and a saturated calomel electrode (SCE) as the reference electrode. The electrolyte was a 3.5 wt.% sodium chloride (NaCl) aqueous solution, prepared from analytical-grade reagents and deionized water. Potentiodynamic polarization scans were initiated after the open-circuit potential (OCP) had stabilized, typically after 30 minutes of immersion. The potential was swept from -250 mV to +250 mV relative to the OCP at a constant scan rate of 1 mV/s. The corrosion potential (E_{corr}) and corrosion current density (i_{corr}) were determined using the Tafel extrapolation method as described in the standard ASTM G102 practice [15-22].

3. RESULTS AND DISCUSSIONS

3.1. Phase Identification and Structural Analysis

3.1.1. X-ray Diffraction Analysis of AISI-201

The phase evolution induced by the CCPN process was meticulously characterized using X-ray diffraction. Figure 1 presents the XRD patterns for both the untreated and nitrided AISI-201 specimens. The diffraction pattern for the untreated substrate is characteristic of a single-phase austenitic (γ-Fe) structure, with prominent peaks corresponding to the (111), (200), and (220) planes of the face-centered cubic (fcc) crystal structure [6]. Following the CCPN treatment at 300°C, a profound transformation in the phase composition is observed. The austenite peaks are substantially diminished in intensity, indicating that the near-surface region has been extensively modified.

The formation of a complex nitride layer is confirmed by the emergence of new diffraction peaks. Most notably, strong peaks corresponding to aluminum nitride (AlN) are identified, which originate from the sputtering of the aluminum cathodic cage and its subsequent reaction with active nitrogen species in the plasma to form a hard, protective coating [17-19]. Concurrently, the detection of chromium nitride (CrN) peaks signifies that a plasma-sample interaction has occurred, leading to the diffusion of nitrogen into the steel substrate and the reaction with chromium from the alloy [9]. The presence of additional peaks suggests the formation of FeN and FeMnN compounds, further corroborating the inward diffusion of nitrogen and its interaction with iron and manganese in the austenitic matrix.

© Ariston Publications 2025. All rights reserved.

The suppression of the CrN phase intensity relative to AlN indicates that the deposition of sputtered material from the cage is a dominant mechanism, with AlN becoming the predominant phase at the surface at this temperature [20-22]. This composite layer of deposited and diffusion-formed nitrides is responsible for the significant enhancement in surface properties.

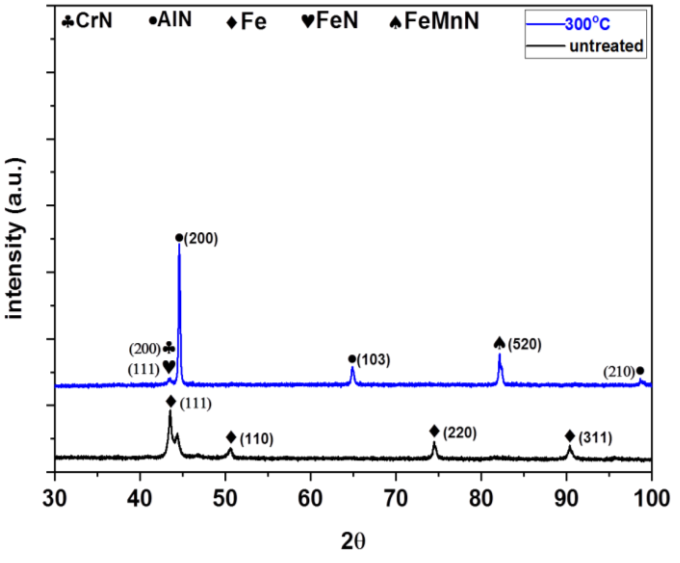


Fig. 1. X-ray diffraction (XRD) pattern of AISI-201 for untreated & nitride at 300°C specimens.

3.1.2. X-ray Diffraction Analysis of Copper

The XRD analysis for copper, presented in Figure 2, reveals an equally significant phase transformation. The pattern for the untreated copper shows the characteristic peaks of pure, crystalline copper. After nitriding at 300°C, this pattern is radically altered. A series of new peaks confirms the successful synthesis of a complex layer structure comprising copper nitrides (Cu_3N, CuN_3, CuN_6), aluminum nitride (AlN), and an intermetallic $AlCu_4$ phase [23]. The appearance of these phases, particularly at a temperature as low as 300°C, is a key finding. Copper is notoriously resistant to nitriding due to its low nitrogen solubility and high activation energy for diffusion; therefore, the formation of a substantial nitride layer is not typically achievable via conventional direct nitriding methods.

The presence of AlN peaks is a direct consequence of the CCPN mechanism, wherein aluminum is sputtered from the cage and deposited onto the copper surface, where it reacts with nitrogen. The formation of various copper nitride phases indicates that active nitrogen species from the plasma have also penetrated the copper lattice, causing expansion and the creation of a metastable nitride structure. The emergence of the $AlCu_4$ peak suggests interdiffusion and reaction between the deposited aluminum and the copper substrate, forming a strong metallurgical bond at the interface. The noticeable peak broadening observed at 300°C is indicative of grain refinement and the introduction of significant microstrain and lattice distortions due to the incorporation of nitrogen atoms, which directly correlates to the hardening effect [24]. The uniformity and intensity of these nitride peaks demonstrate the efficacy and consistency of the CCPN process in modifying the copper surface.

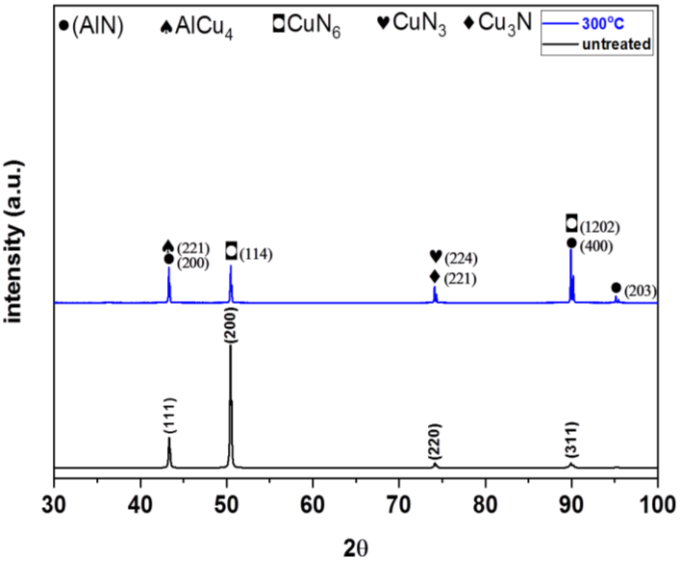


Fig. 2. Graphical representation of Cu for untreated and nitrided at 300°C specimens.

3.2. Microhardness Evolution

3.2.1. Hardness Profile of AISI-201

The microhardness profiles, as a function of applied load, for the untreated and nitrided AISI-201 samples are graphically represented in Figure 3(a). The untreated specimen exhibits a characteristic low hardness of approximately 200 HV, which is typical for annealed austenitic stainless steel. In stark contrast, the sample treated at 300°C demonstrates a remarkable increase in surface hardness, achieving a maximum value of ~620 HV at the lowest applied load. This represents an enhancement of roughly 300% compared to the base material.

This dramatic improvement in hardness is directly attributable to the complex nitride layer identified by XRD. The dispersion of hard ceramic phases like AlN and CrN within the near-surface region creates a composite structure that strongly resists plastic deformation under the indenter [4]. Furthermore, the dissolution of interstitial nitrogen atoms into the austenitic lattice causes significant lattice strain and solid solution strengthening, contributing to the overall hardening effect. The hardness values exhibit a gradual decline with increasing applied load, which is a standard phenomenon as the indentation penetrates deeper into the material, sampling a larger volume that includes the softer substrate beneath the hardened layer. Even at the maximum load of 1000 gf, the measured hardness remains significantly higher than that of the untreated material, confirming that the nitrided case depth is sufficient to provide mechanical

© Ariston Publications 2025. All rights reserved.

support to the hard outer layer. The calculated indentation depth at this load correlates well with an estimated case depth of over 13 µm.

3.2.2. Hardness Profile of Copper

The results for copper, shown in Figure 3 (b), are even more pronounced. The soft nature of pure copper is evidenced by the low hardness of ~90 HV for the untreated sample. After CCPN treatment at 300°C, the surface hardness skyrockets to approximately 965 HV, representing an increase of over 900%. This extraordinary enhancement is a consequence of the multifaceted strengthening mechanisms activated by the process. The formation of a coherent layer containing hard copper and aluminum nitride phases (Cu_3N, AlN) and the intermetallic $AlCu_4$ compound provides immense dispersion strengthening [17]. Simultaneously, the forced introduction of nitrogen interstitials into the copper crystal structure, which has very limited solubility, induces severe lattice distortions and a potent solid solution strengthening effect. The hardness profile shows a sharp gradient with increasing load, indicative of a relatively thin but extremely hard nitride layer. The hardness value decreases rapidly as the indenter penetrates beyond this layer into the unaffected, soft copper substrate. The depth of the indentation at 1000 gf corresponds to a layer thickness of approximately 14 µm, which is consistent with the formation of a well-defined, thin-film composite structure on the surface.

3.3. Surface Morphology and Elemental Composition

3.3.1. Scanning Electron Microscopy of AISI-201

The surface morphology of the samples was investigated using scanning electron microscopy. Figure 4 (a) shows the untreated AISI-201 sample, which displays a uniform surface with fine, parallel scratching from the final polishing step. Figure 4 (b) reveals the dramatic morphological change after CCPN treatment at 300°C. The surface is now covered with a dense, homogeneous layer of deposited material. A distinctive feature observed at higher magnification is the presence of nanoscale, rice-like structures embedded within the matrix. These structures are indicative of ferrite (α-Fe) nanostructures that have precipitated during the nitriding process, a phenomenon that has been documented in literature and can influence both mechanical and chemical properties [25]. The surface is devoid of the polishing scratches, which have been effectively obscured by the deposited nitride layer, confirming the uniformity and completeness of the surface coverage.

3.3.2. Energy Dispersive X-ray Spectroscopy of AISI-201

The EDS analysis, presented in Figure 5, provides quantitative elemental evidence of the surface modification. The spectrum from the untreated sample (Figure 5 (a)) shows the expected constituents of AISI-201, iron, chromium, manganese, and nickel, along with minor traces of silicon and carbon from polishing residues. The spectrum from the nitrided sample (Figure 5 (b)) is markedly different. A strong nitrogen peak is present, confirming successful nitriding. A significant aluminum peak is also detected, providing direct evidence of the sputtering and deposition from the aluminum cathodic cage. The persistence of iron, chromium, and manganese peaks confirms that the nitride layer is not a pure AlN film but a composite structure where diffusion from the substrate has occurred, supporting the XRD findings of CrN and FeMnN formation.

3.3.3. Scanning Electron Microscopy of Copper

The SEM micrographs for copper are shown in Figure 6. The untreated surface (Figure 6 (a)) is smooth with visible polishing grooves. After nitriding (Figure 6 (b)), the surface morphology is completely transformed into a uniform, granular structure comprised of fine, agglomerated particles.

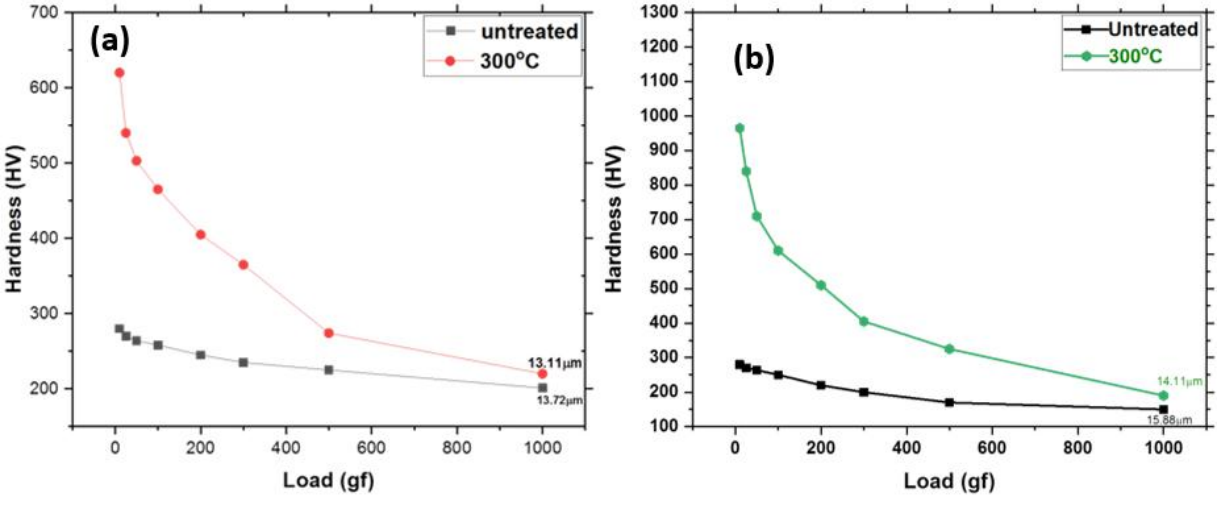


Fig. 3. Microhardness of untreated and 300°C nitrided (a) AISI-201 and (b) copper samples.

© Ariston Publications 2025. All rights reserved.

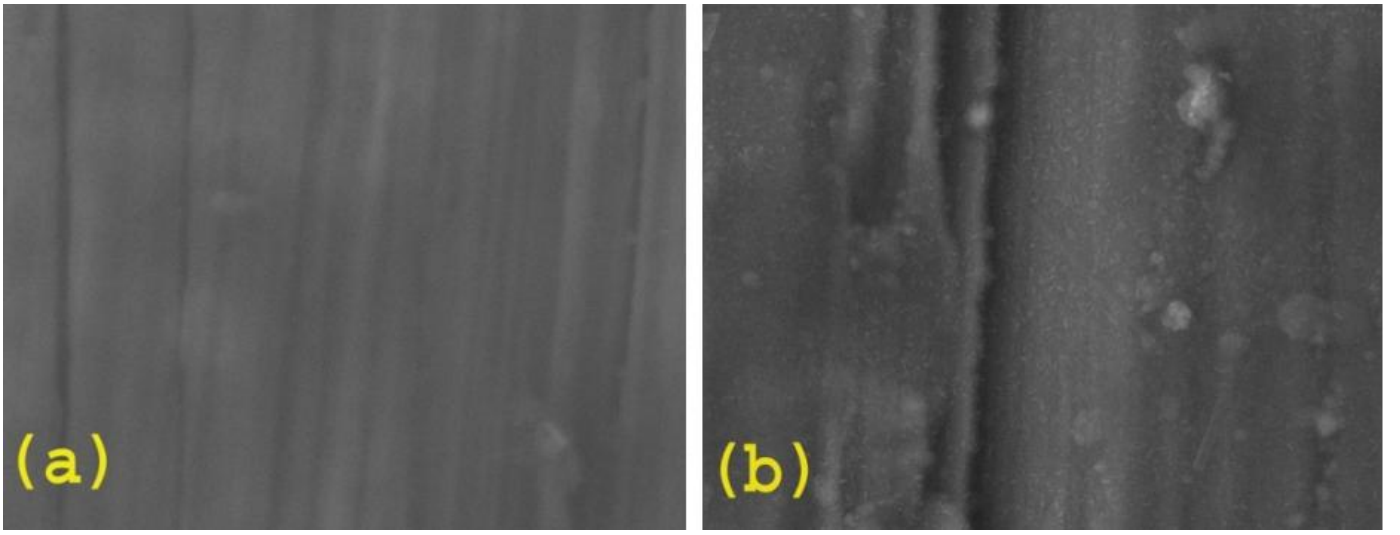


Fig. 4. SEM analysis of AISI-201 of (a) untreated (b) 300°C nitrided specimens.

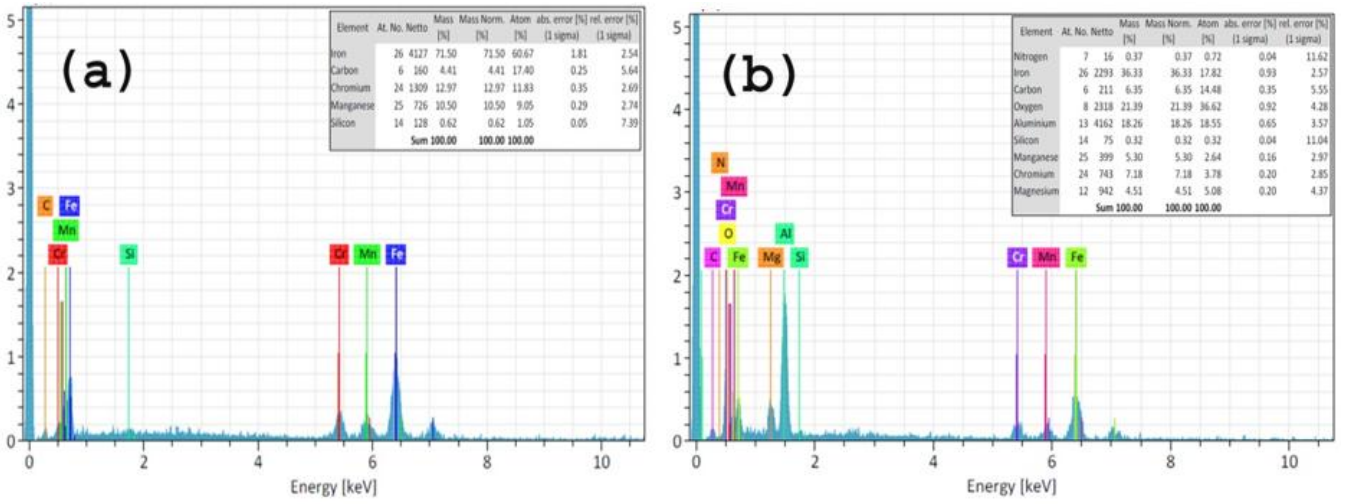


Fig. 5. EDS analysis of AISI-201 of (a) untreated and (b) 300°C nitrided specimen.

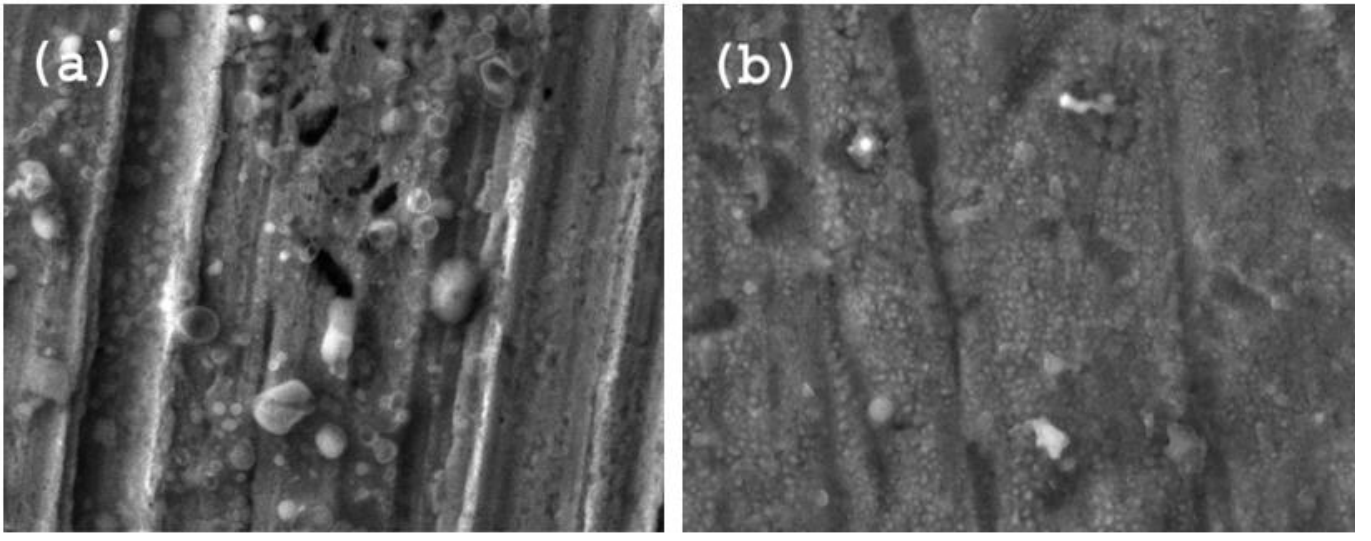


Fig. 6. SEM analysis of Copper (a) untreated (b) 300°C nitrided specimens.

© Ariston Publications 2025. All rights reserved.

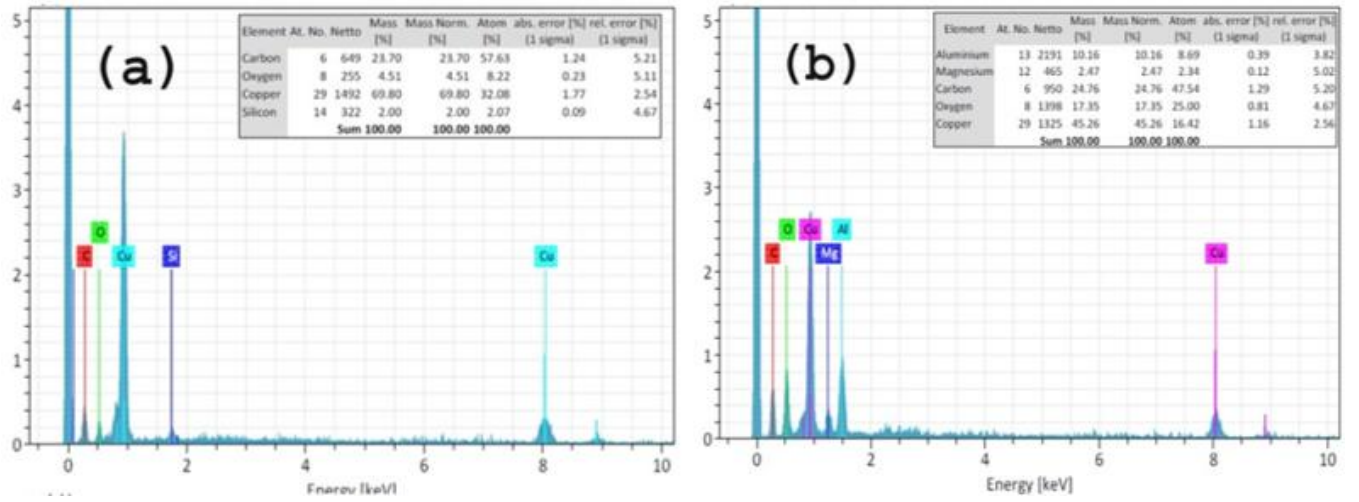


Fig. 7. EDS analysis of Copper of (a) untreated and (b) 300°C nitrided specimen.

These particles are clusters of aluminum and copper nitrides, which have nucleated and grown on the surface during the CCPN process [17-20]. The coating appears continuous and well-adhered, with no evidence of cracking or delamination, which is crucial for tribological applications.

3.3.4. Energy Dispersive X-ray Spectroscopy of Copper

The EDS results for copper, Figure 7, corroborate the XRD and SEM findings. The untreated sample spectrum (Figure 7 (a)) shows only copper, with oxygen, carbon, and silicon present as surface contaminants. The spectrum from the nitrided sample (Figure 7 (b)) is dominated by strong nitrogen and aluminum peaks, alongside the substrate copper signal. The presence of aluminum and nitrogen confirms the deposition of AlN, while the persistence of the copper peak indicates that the layer is thin enough for the electron beam to penetrate to the substrate, or that copper nitrides are present at the surface. The complete absence of silicon suggests that the nitride layer has fully covered the original surface impurities.

3.4. Electrochemical Corrosion Behavior

3.4.1. Potentiodynamic Polarization of AISI-201

The corrosion resistance of the materials was evaluated in a 3.5 wt.% NaCl solution using potentiodynamic polarization, with the curves presented in Figure 8 (a). The Tafel extrapolation technique is utilized to assess the corrosion potential, corrosion current density, Tafel constants and corrosion rates. The typical Stern-Geary equation [26] is utilized to find out polarization resistance.

$$R_p = \frac{\beta_A \beta_C}{2.303 i_{corr}(\beta_A + \beta_C)}$$

The cathodic β provides the least value for the untreated sample while the anodic β exhibits an almost straight line trend in its inverse relationship with the temperature. With the exception of the untreated sample, the treated samples show an increase in E_{corr} when compared to the untreated sample; it means the nitrided sample has better corrosion resistance. The formation of the rice like nanostructures affects the overall trend of I_{corr} and $E_{corr.}$ for samples treated at temperatures 300°C. The untreated AISI-201 sample exhibits active corrosion behavior with a relatively negative corrosion potential (E_{corr}) and a higher corrosion current density (i_{corr}). The nitrided sample shows a clear shift in the polarization curve. The E_{corr} value is shifted to a more noble (positive) potential, and the i_{corr} is significantly reduced.

This improvement in corrosion resistance is attributed to the protective nature of the continuous nitride layer, which acts as a physical barrier isolating the underlying steel from the corrosive electrolyte. The formation of a stable AlN and CrN layer prevents the aggressive chloride ions from initiating pitting corrosion on the otherwise vulnerable austenitic substrate. However, it is noted that the corrosion rate does not improve as dramatically as the mechanical properties. This can be attributed to the complex microstructure of the layer; the presence of Mn (known to sometimes reduce corrosion resistance in stainless steels) and the aforementioned rice-like nanostructures might create localized micro-galvanic cells, slightly offsetting the overall beneficial barrier effect of the nitride layer [26]. Nonetheless, the net effect is an improvement in corrosion performance.

3.4.2. Potentiodynamic Polarization of Copper

The polarization curves for copper are shown in Figure 8(b). The untreated copper undergoes active corrosion with a high corrosion rate. The nitrided sample, however, demonstrates superior corrosion performance. Its polarization curve is characterized by a more noble E_{corr} and a passivation-like behavior, evidenced by a region where the current density

© Ariston Publications 2025. All rights reserved.

remains relatively constant despite an increase in potential. This indicates that the nitride layer (AlN and copper nitrides) is not merely a barrier but is itself stable in the chloride environment, effectively passivating the surface and drastically reducing the corrosion rate.

3.5. Tribological Performance

3.5.1. Wear Track Analysis of AISI-201

The wear resistance was assessed by analyzing the wear tracks post ball-on-disc testing. Figure 9(a) shows the wear scar on the untreated AISI-201 sample. It is characterized by a wide, deep track with severe plastic deformation, adhesive material transfer, and grooving, indicative of abrasive and adhesive wear mechanisms. This is a direct consequence of the material's low surface hardness. In contrast, the wear track on the nitrided sample (Figure 9 (b)) is exceptionally shallow and narrow. The surface is smooth with only mild polishing wear, and there is no evidence of plowing or adhesion. The hard nitride layer effectively resisted penetration and plastic deformation, leading to a transition from severe wear to mild wear mode [15-18].

3.5.2. Wear Track Analysis of Copper

A similar contrast is observed for copper, as shown in Figure 10. The untreated copper (Figure 10 (a)) suffered catastrophic wear, with a deep, gouged track and extensive material removal. The nitrided sample (Figure 10 (b)) exhibited outstanding wear resistance. The wear track is barely visible under SEM, appearing as a slight polish on the surface, with no measurable material loss. The transformation from a soft, ductile metal to a hard, wear-resistant surface composite is unequivocally demonstrated.

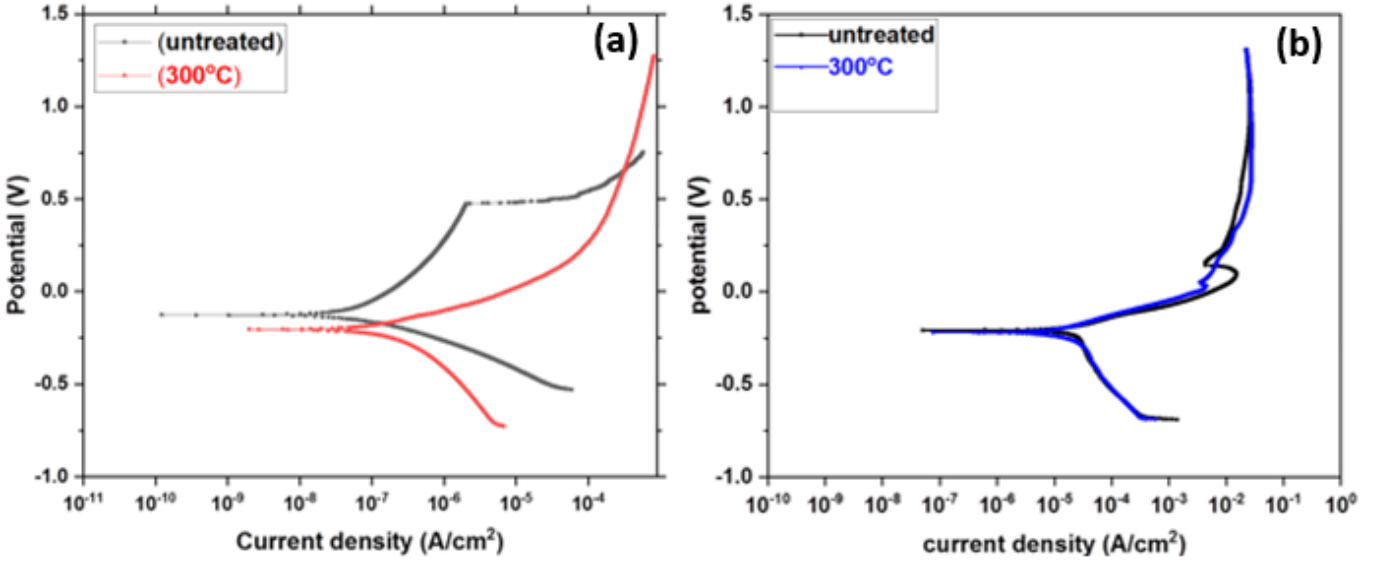


Fig. 8. Analysis of potentiodynamic polarization curve of (a) AISI-201 and (b) Copper.

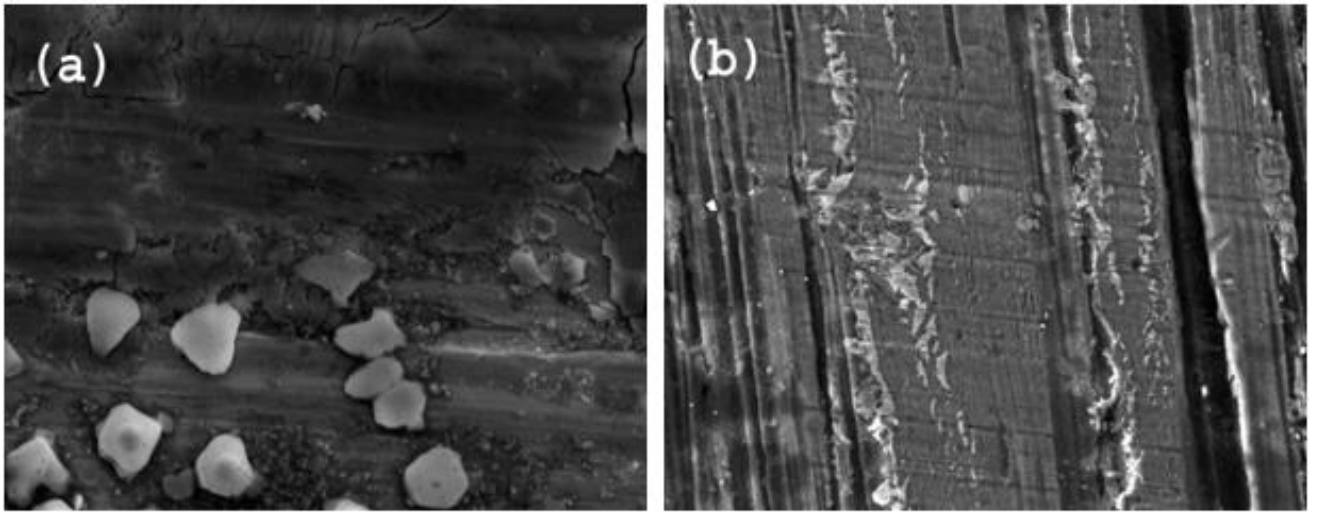


Fig. 9. Wear analysis of AISI-201 with SEM (a) untreated (b) nitrided at 300°C.

© Ariston Publications 2025. All rights reserved.

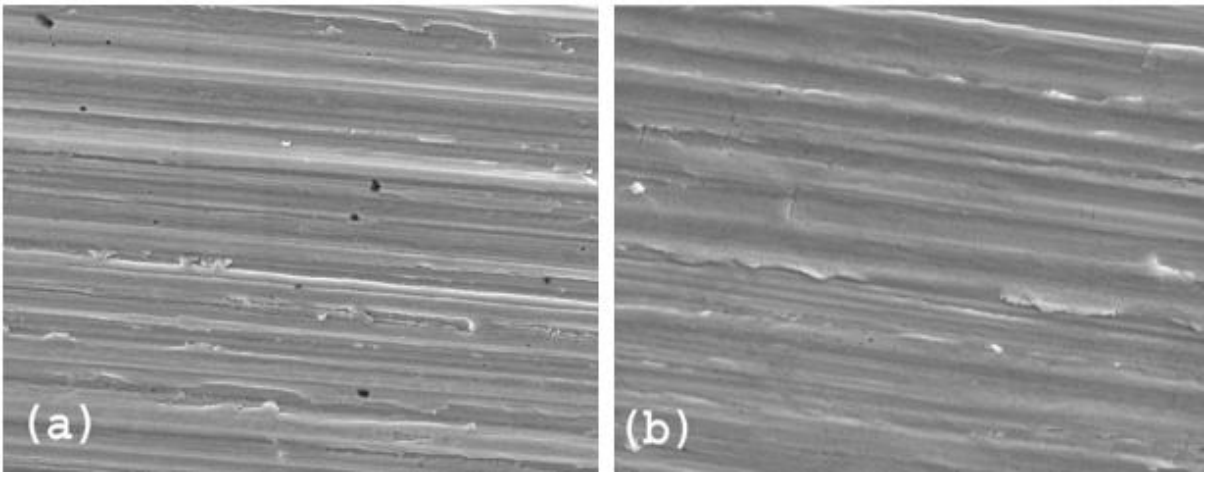


Fig. 10. Wear analysis of Copper with SEM (a) untreated (b) nitrided at 300°C.

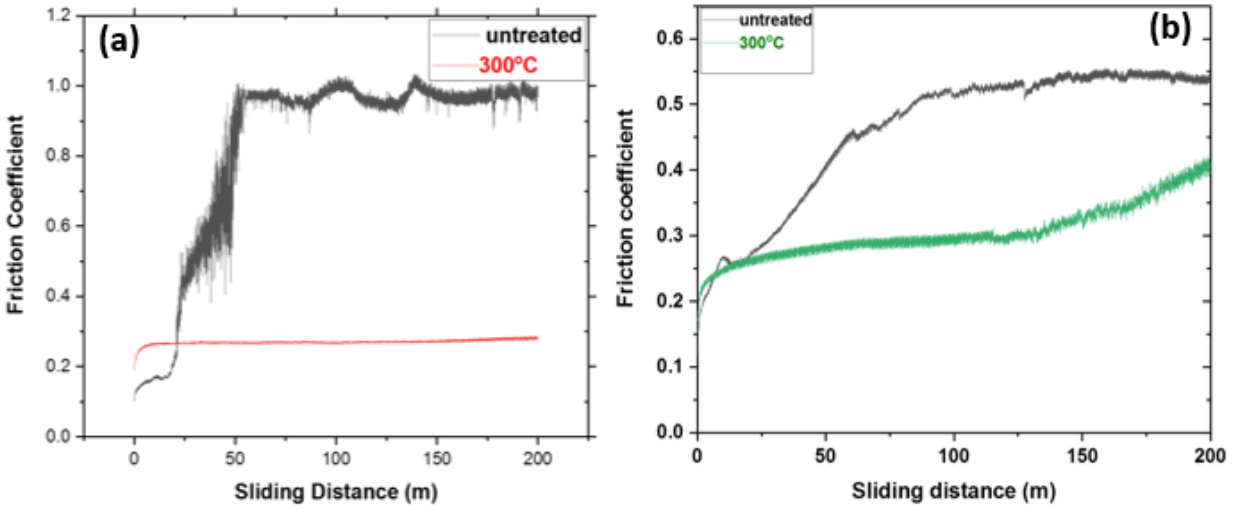


Fig. 11. Friction coefficient of (a) AISI-201 and (b) copper.

3.5.3. Coefficient of Friction

The friction coefficients during sliding are plotted in Figure 11. For both AISI-201 (Figure 11 (a)) and copper (Figure 11 (b)), the untreated materials exhibit high and fluctuating coefficients of friction, consistent with their soft nature, adhesion to the counterface, and severe wear. The nitrided samples, however, display a significantly lower and stable coefficient of friction. This is due to the combination of high surface hardness, which reduces plastic deformation and plowing, and the possible lubricious nature of some of the nitride phases formed [17, 24]. The stable, low friction further confirms the exceptional tribological performance of the CCPN-treated surfaces.

4. CONCLUSION

This study conclusively demonstrates that cathodic cage plasma nitriding (CCPN) with an aluminum cage is a highly effective technique for significantly enhancing the surface properties of AISI-201 austenitic stainless steel and copper at a relatively low temperature of 300°C. The research successfully addressed the inherent challenges associated with nitriding these materials; AISI-201, being an austenitic steel, is typically prone to the formation of chromium-depleted zones that impair corrosion resistance, while copper does not readily form stable nitrides through conventional means. The CCPN process overcame these limitations by facilitating the deposition of a hard, complex nitride layer. The formation of phases such as AlN, CrN, FeN, and FeMnN on the stainless steel and AlN, various copper nitrides (Cu_3N, CuN_3, CuN_6), and an intermetallic $AlCu_4$ phase on copper was unequivocally confirmed through XRD analysis. This microstructural transformation was the fundamental driver for the dramatic improvement in mechanical and chemical properties. The surface hardness experienced a threefold increase, a direct consequence of solid solution strengthening and the dispersion of hard nitride compounds. This superior hardness directly translated into exceptional wear performance. The nitrided layers exhibited a significantly

© Ariston Publications 2025. All rights reserved.

lower coefficient of friction and much shallower, narrower wear tracks compared to the soft, susceptible untreated surfaces, indicating a transition from severe adhesive and abrasive wear to a much milder wear regime. Furthermore, the potentiodynamic polarization tests revealed improved corrosion resistance for the nitrided samples. The formation of a stable, protective nitride layer acted as a barrier against the corrosive chloride ions in the solution, leading to a more noble corrosion potential and a reduced corrosion current density. The synergy between improved hardness, wear resistance, and corrosion performance positions the CCPN-treated AISI-201 and copper as far more suitable for demanding industrial applications such as bearing surfaces, marine components, and electrical contacts. The success of using an aluminum cathodic cage opens avenues for using alternative cage materials to deposit different hard coatings. Future work could explore a wider range of temperatures and durations to optimize the layer thickness and phase composition, further pushing the boundaries of performance for these enhanced materials.

DECLARATIONS

Ethical Approval

We affirm that this manuscript is an original work, has not been previously published, and is not currently under consideration for publication in any other journal or conference proceedings. All authors have reviewed and approved the manuscript, and the order of authorship has been mutually agreed upon.

Funding

Not applicable

Availability of data and material

All of the data obtained or analyzed during this study is included in the report that was submitted.

Conflicts of Interest

The authors declare that they have no financial or personal interests that could have influenced the research and findings presented in this paper. The authors alone are responsible for the content and writing of this article.

Author's contribution statement

All authors contributed equally to this work.

REFERENCES

[1] Souza Filho, I.R., Sandim, M.J.R., Cohen, R., Nagamine, L.C.C.M., Hoffmann, J., Bolmaro, R.E. and Sandim, H.R.Z., **2016**. Effects of strain-induced martensite and its reversion on the magnetic properties of AISI 201 austenitic stainless steel. *Journal of Magnetism and Magnetic Materials*, 419, pp.156-165.

[2] Padilha, A.F., Plaut, R.L. and Rios, P.R., **2003**. Annealing of cold-worked austenitic stainless steels. *ISIJ International*, 43, pp.135-143.

[3] Zhang, L., Takahashi, S., Kamada, Y., Kikuchi, H., Ara, K., Sato, M. and Tsukada, T., **2005**. Magnetic properties of SUS 304 austenitic stainless steel after tensile deformation at elevated temperatures. *Journal of Materials Science*, 40, pp.2709-2711.

[4] Gao, Y. and Zheng, S., **2016**. Effect of Plasma Nitriding Temperatures on Characteristics of Aisi 201 Austenitic Stainless Steel. *Surface Review and Letters*, 23, p.1550084.

[5] Lee, I., **2012**. Effect of processing temperatures on characteristics of surface layers of low temperature plasma nitrocarburized AISI 204Cu austenitic stainless steel. *Transactions of Nonferrous Metals Society of China*, 22, pp.s678-s682.

[6] Mangonon, P.L. and Thomas, G., **1970**. The martensite phases in 304 stainless steel. *Metallurgical Transactions*, 1, pp.1577-1586.

[7] Bowkett, M.W., Keown, S.R. and Harries, D.R., **1982**. Quench-and deformation-induced structures in two austenitic stainless steels. *Metal Science*, 16, pp.499-518.

[8] Mumtaz, K., Takahashi, S., Echigoya, J., Kamada, Y., Zhang, L.F., Kikuchi, H. and Sato, M., **2004**. Magnetism and microstructure of martensite in plastically deformed 304 austenitic stainless steel. *Journal of Materials Science*, 39, pp.85-97.

[9] Choi, J.Y. and Jin, W., **1997**. Strain induced martensite formation and its effect on strain hardening behavior in the cold drawn 304 austenitic stainless steels. *Scripta Materialia*, 36, pp.99-104.

[10] Güler, E., Kirindi, T. and Aktas, H., **2007**. Comparison of thermally induced and deformation induced martensite in Fe–29% Ni–2% Mn alloy. *Journal of Alloys and Compounds*, 440, pp.168-172.

[11] Thankachan, T. and Prakash, K.S., **2017**. Microstructural, mechanical and tribological behavior of aluminum nitride reinforced copper surface composites fabricated through friction stir processing

 © Ariston Publications 2025. All rights reserved.

route. *Materials Science and Engineering: A*, 688, pp.301-308.

[12] Taweesub, K., Visuttipitukul, P., Tungkasmita, S. and Paosawatyanyong, B., **2010**. Nitridation of Al–6% Cu alloy by RF plasma process. *Surface and Coatings Technology*, 204, pp.3091-3095.

[13] Visuttipitukul, P., Aizawa, T. and Kuwahara, H., **2003**. Feasibility of plasma nitriding for effective surface treatment of pure aluminum. *Materials Transactions*, 44, pp.1412-1418.

[14] ASM Handbook, **1993**. Aluminum and aluminum alloys. *ASM International*, 14.

[15] Naeem, M., Shafiq, M., Zaka-ul-Islam, M., Díaz-Guillén, J.C., Lopez-Badillo, C.M., Ullah, N. and Zakaullah, M., **2017**. Improved surface properties of AISI-304 by novel duplex cathodic cage plasma nitriding. *Materials Letters*, 189, pp.213-216.

[16] Naeem, M., Iqbal, J., Shabbir, F., Khan, M.A., Díaz-Guillén, J.C., Lopez-Badillo, C.M. and Shafiq, M., **2019**. Effect of pulsed current on cathodic cage plasma nitriding of non-alloyed steel. *Materials Research Express*, 6, p.086537.

[17] Naeem, M., Shafiq, M., Zaka-ul-Islam, M., Ashiq, A., Díaz-Guillén, J.C., Shahzad, M. and Zakaullah, M., **2016**. Enhanced surface properties of plain carbon steel using plasma nitriding with austenitic steel cathodic cage. *Materials & Design*, 108, pp.745-753.

[18] Naeem, M., Shafiq, M., Zaka-ul-Islam, M., Díaz-Guillén, J.C., Lopez-Badillo, C.M., Ullah, N. and Zakaullah, M., **2017**. Improved surface properties of AISI-304 by novel duplex cathodic cage plasma nitriding. *Materials Letters*, 189, pp.213-216.

[19] Naeem, M., Shafiq, M., Zaka-ul-Islam, M., Nawaz, N., Díaz-Guillén, J.C. and Zakaullah, M., **2016**. Effect of cathodic cage size on plasma nitriding of AISI 304 steel. *Materials Letters*, 181, pp.78-81.

[20] Naeem, M., Khattak, Z.I., Zaka-ul-Islam, M., Shabir, S., Khan, A.W. and Zakaullah, M., **2014**. Investigation of plasma parameters in an active screen cage-pulsed dc plasma used for plasma nitriding. *Radiation Effects and Defects in Solids*, 169, pp.893-905.

[21] Naeem, M., Raza, H.A., Shafiq, M., Zaka-ul-Islam, M., Iqbal, J., Díaz-Guillén, J.C. and Zakaullah, M., **2017**. Effect of pulsed duty cycle control on tribological and corrosion properties of AISI-316 in cathodic cage plasma nitriding. *Materials Research Express*, 4, p.116507.

[22] Naeem, M., Raza, H.A., Shafiq, M., Shabbir, F., Iqbal, J., Diaz-Guillen, J.C. and Lopez-Badillo, C.M., **2019**. Improved nitriding capability of nonalloyed steels assisted with active screen plasma treatment. *Surface Review and Letters*, 26, p.1950118.

[23] Nowakowska-Langier, K., Chodun, R., Minikayev, R., Okrasa, S., Strzelecki, G.W., Wicher, B. and Zdunek, K., **2018**. Phase composition of copper nitride coatings examined by the use of X-ray diffraction and Raman spectroscopy. *Journal of Molecular Structure*, 1165, pp.79-83.

[24] Bashir, M.I., Shafiq, M., Naeem, M., Zaka-ul-Islam, M., Díaz-Guillén, J.C., Lopez-Badillo, C.M. and Zakaullah, M., **2017**. Enhanced surface properties of aluminum by PVD-TiN coating combined with cathodic cage plasma nitriding. *Surface and Coatings Technology*, 327, pp.59-65.

[25] Sohn, Y., Pradhan, D., Kang, J.S. and Leung, K.T., **2015**. Nanoscale architecture of bimetallic hybrid Fe–Au nanostructures with and without 1, 4-phenylene diisocyanide pre-functionalization. *RSC Advances*, 5, pp.31472-31478.

[26] Yazıcı, M., Çomaklı, O., Yetim, T. and Yetim, A.F., **2015**. The effect of plasma nitriding temperature on the electrochemical and semiconducting properties of thin passive films formed on 316 L stainless steel implant material in SBF solution. *Surface and Coatings Technology*, 261, pp.181-188.

© Ariston Publications 2025. All rights reserved.